### Title

Magnetic resonance imaging provides spatial resolution of Chilling Injury in Micro-Tom tomato (Solanum lycopersicum L.) fruit




### Authors

Tao, Fei
Zhang, Lu
McCarthy, Michael J
et al.



### Publication Date

2014-11-01

### DOI

10.1016/j.postharvbio.2014.06.005

Peer reviewed

Postharvest Biology and Technology 97 (2014) 62–67

Contents lists available at ScienceDirect

Postharvest Biology and Technology

journal homepage: www.elsevier.com/locate/postharvbio

# Magnetic resonance imaging provides spatial resolution of Chilling Injury in Micro-Tom tomato (*Solanum lycopersicum* L.) fruit

Fei Tao[a,d], Lu Zhang[b], Michael J. McCarthy[b,c], Diane M. Beckles[a,*], Mikal Saltveit[a]

[a] Department of Plant Sciences, University of California, One Shields Avenue, Davis, CA 95616, United States
[b] Department of Food Science and Technology, University of California, One Shields Avenue, Davis, CA 95616, United States
[c] Department of Biological and Agricultural Engineering, University of California, One Shields Avenue, Davis, CA 95616, United States
[d] Food Science Institute, Zhejiang Academy of Agricultural Sciences, Hangzhou 310021, China

ARTICLE INFO

*Article history:*
Received 20 February 2014
Accepted 4 June 2014

*Keywords:*
Chilling injury
Tomato fruit
Magnetic resonance imaging (MRI)
Apparent diffusion coefficient (ADC)

ABSTRACT

Magnetic resonance imaging (MRI) was used to monitor internal changes in harvested tomato (*Solanum lycopersicum* L. cv. Micro-Tom) fruit. Measurements of ethylene evolution, respiration, and ion leakage indicated that the fruit developed chilling injury (CI) after storage at 0 °C. Unlike these measurements, MRI provided spatially resolved data. The apparent diffusion coefficient (ADC), which is an indication of water mobility in tissues, was calculated from MRIs of the different parts of the fruit. Storage for 1 or 2 weeks at 0 °C caused no difference in the ADCs (*D*-values) in the pericarp, but it did lead to higher values in the inner tissues i.e., the columella and locular region compared to non-chilled fruit ($P < 0.05$). Changes in inner fruit *D*-values after 1 and 2 weeks of chilling at 0 °C were similar to changes in respiration, ethylene production and ion leakage which increased ($P < 0.05$) compared to the non-chilled controls. Most CI studies of tomato fruit used pericarp tissue. Our data indicate that columella tissue changes occur in response to chilling injury in tomato fruit and suggest that more caution is needed when interpreting data from experiments commonly used to study this phenomenon.



## 1. Introduction

Exposure of susceptible plant tissues to non-freezing temperatures below 10–12 °C induces a physiological disorder called Chilling Injury (CI) (Saltveit, 2000, 2005). There appears to be two phases in the development of CI. The first phase is initiated in the cold (Lyons, 1973) and could involve a change in membrane fluidity or enzyme activity (Saltveit, 2000). Overt symptoms develop after prolonged chilling or upon warming to non-chilling temperatures (e.g., 20 °C) (Saltveit, 2000, 2003). These secondary symptoms are predicated by primordial events initiated in the cold, and include a host of metabolic and physiological changes that include increased membrane permeability (Saltveit, 2005), increased respiration and ethylene production (Saltveit, 2003), uneven ripening, disease susceptibility, water soaking and surface pitting (Luengwilai et al., 2012a; Morris, 1982; Sharom et al., 1994). A technique that could detect the earliest physiological changes associated with CI would foster a better understanding of the initial events leading to this disorder, and point to more effective ameliorative action.

Magnetic resonance imaging (MRI) is a nondestructive imaging technique, which is increasingly used to visualize and quantify fruit physiological response to endogenous or exogenous stimuli (Abbott, 1999; Defraeye et al., 2013). MRI uses the magnetic properties of nuclei and their interactions with radio frequency and applied magnetic fields to produce an image (Clark et al., 1997). Variations in the chemical composition and integrity of cellular structures can change the movement of water within and among tissues. These changes can be detected as modifications in the relaxation times of the protons in water, which in turn alters the signals used to construct MR images (Zhang and McCarthy, 2012). Diffusion-weighted MRI of tissues provides a quantitative measure (*D*-values) of the apparent diffusion coefficient of water, instead of estimations of water mobility from relaxation measurement that include the influence of translational mobility, composition and other factors (Zhang and McCarthy, 2012). In addition, a spatially resolved map of the apparent diffusion coefficient (ADC) of water can be obtained, which could help to understand and quantify the development of disorders such as CI within the tissue.

MRI has been used to gain insight into early phases of different postharvest physiological disorders before the manifestation

* Corresponding author at: Department of Plant Sciences MS3, University of California, Davis, CA 95616, United States. Tel.: +1 530 754 4779.
*E-mail address:* dmbeckles@ucdavis.edu (D.M. Beckles).

http://dx.doi.org/10.1016/j.postharvbio.2014.06.005
0925-5214/

of external symptoms (Nicolai et al., 2014). These include core breakdown in pear (Lammertyn et al., 2003) watercore disorder (Herremans et al., 2014), internal browning (Gonzalez et al., 2001) and mealiness in apple (Barreiro et al., 1999; Letal et al., 2003). There are few reports where MRI was used to detect the early stages of CI in sensitive produce. In persimmon, MR images of cold-stored fruit were distinct from those stored at ambient temperature (Clark and Forbes, 1994). In zucchini squash (Wang and Wang, 1992), MRI provided enough data to act as a predictor of where water soaking would occur in the epidermis after the cold-storage. These studies both indicated that MRI has great potential for studying CI in fruit tissues.

Tomato (*Solanum lycopersicum* L.) is one of the most important horticultural crops both economically (Beckles et al., 2012) and as a genomics, molecular, biochemical, and physiological model for biological processes occurring in fleshy fruits (Seymour et al., 2013). Like most subtropical fruit, tomato is susceptible to CI. Studies with tomato fruit could leverage existing functional genomics resources to pinpoint the molecular basis of this trait. To our knowledge, MRI has not been used to study CI in this species. We used the dwarf cultivar 'Micro-Tom' because it is the functional genomics model for tomato (Meissner et al., 1997). Its high-density growth, short life cycle and concentrated fruit-set (i.e., many fruit of a similar age) makes it possible to obtain harvests of 500 fruit or more per square meter per year (Meissner et al., 1997). Because tomato postharvest studies can be hampered by biological variability (Hertog et al., 2004), the availability of numerous, similarly aged fruit makes Micro-Tom a convenient experimental model for postharvest studies (Gomez et al., 2009; Luengwilai et al., 2012a,b; Malacrida et al., 2006; Re et al., 2012; Sorrequieta et al., 2013; Vega-Garcia et al., 2010; Weiss and Egea-Cortines, 2009). Furthermore, we have previously characterized Micro-Tom fruit physiological response to a range of postharvest chilling temperature-time combinations (Luengwilai et al., 2012a), and used this information to design a metabolomics investigation of CI (Luengwilai et al., 2012b). This has established a baseline with this cultivar for the further CI studies we exploit here.

The specific objective of this study was to determine if MRI could detect some of the earliest physiological changes that accompany CI in tomato fruit. Current methods of assessing the occurrence and severity of CI are: (1) time consuming (e.g., enzyme assays, carbon dioxide and ethylene production), (2) destructive (e.g., measurement of ion leakage from excised tissue, firmness tests), or (3) occur only after the activation of secondary, downstream events (e.g., the CI index). These methods are time-proven and are indispensable, but there is a need for non-destructive methods with equivalent or better sensitivity to those currently used. MRI potentially offers such advantages and could be an important complementary tool for studying incipient CI. We show that MRI can provide spatio-temporal resolution of chilling induced changes in Micro-Tom tomato fruit prior to development of downstream symptoms.

## 2. Materials and methods

### 2.1. Plant growth conditions

Tomato (*S. lycopersicum* L. cv. Micro-Tom) seeds were a gift from Dr. David Weiss (The Hebrew University of Jerusalem, Israel). Tomato plants were grown from May to August 2012 in greenhouses located in Davis, CA as previously described (Luengwilai et al., 2012a).

### 2.2. Fruit sampling and postharvest treatments

Mature green fruit were hand-harvested between 7 and 8 am (Saltveit, 1991). Unblemished fruit that were both uniform in size and external color were washed in commercial bleach (1:20 dilution of 5% (v/v) sodium hypochlorite) and allowed to dry in a transfer hood. A total of 12 fruit were used in each of the four treatments. Control fruit were held at 20 °C, while the remaining treatments were as follows: (1) 0 °C for 1 week, (2) 0 °C for two weeks, and (3) 0 °C for 2 weeks followed by storage at 20 °C for an additional week.

### 2.3. Respiration rate and ethylene production

Chilled fruit were removed from 0 °C and allowed to slowly (2–3 h) warm to 20 °C before $CO_2$ and ethylene production were measured. Twelve fruit were evaluated per treatment by placing four fruit in each of three 500 mL glass containers. These jars were sealed for 1 h and a 1-mL sample of the head space was withdrawn using a syringe and its $CO_2$ concentration was measured with an infrared gas analyzer as previously described (Saltveit and Strike, 1989). Ethylene production was measured from a 2.5 mL sample of the head-space using a Gas Chromatograph (Model Carle 211, Hach Carle, Loveland, CO) equipped with a flame ionization detector. These two samples were taken within 30 s of each other from the same jar.

### 2.4. Ion leakage measurement

Each fruit was cut into four radial segments, cleaned of adhering locular tissue, washed for 5 s in running tap water, blotted dry, and one segment was placed in each sector of a 4-sectored Petri dish under aseptic conditions. The dishes were placed in plastic tubs lined with wet paper towels and loosely covered with aluminum foil. The tubs were held at 12.5 °C for 18 h to produce 'aged' tissue, i.e., to allow the tissue to overcome the wound-induced alterations in membrane permeability (Saltveit, 2005). After transferring to room temperature (~18 °C) for 1 h, the four aged segments from each Petri dish were put into a 50 mL plastic centrifuge tube containing 20 mL of an aqueous solution of 0.2 M mannitol. Preliminary experiments determined that 0.2 M was isotonic for these excised radial segments (Saltveit, 2005)

The conductivity of the bathing solution was measured with an Extech Model 480 digital conductivity meter (Waltham, MA) every 5 min for 30 min and then less frequently for 180 min with gently shaken between readings. After 3 h the tubes were capped, frozen at −20 °C and warmed to room temperature and frozen and thawed twice before the total conductivity of the solution was measured at room temperature after 1 h of shaking. Ion leakage was expressed as percent of total and plotted over time. The linear increase in ion leakage from 0.5 to 2.0 h was used to calculate the rate of ion leakage (Saltveit, 2002, 2005).

### 2.5. MR imaging and data acquisition

MRI data were acquired on a 1 T permanent magnet NMR spectrometer (Aspect Imaging, Industrial Area Hevel Modi'in, Shoham, Israel) with a 60 mm inside diameter (ID) coil. Each tomato fruit was positioned at the center of the coil during imaging. A diffusion weighted spin echo (SE-DW) imaging sequence was used to obtain the image of the equatorial slice of the sample. A set of 12 images for each sample was acquired with a series of motion-encoding gradients composed of 12 steps ($b$ in Eq. (1)), applied in the spin echo sequence with a repetition time (TR) of 1000 ms, an echo time (TE) of 30 ms, field of view (FOV) of 64 mm × 64 mm, and slick thickness of 2 mm. In the SE-DW images, the signal intensity (S) of any voxel is given as:

$$S = S_0 e^{-bD} \quad (1)$$

$$b = \gamma^2 G^2 \delta^2 \left( \Delta - \frac{\delta}{3} \right) \quad (2)$$

where $S_0$ is the signal intensity of the spin echo image without any diffusion gradient ($b = 0\ s/mm^2$), $D$ is the apparent diffusion coefficient (ADC). The diffusion weighting factor $b$ is a function of the gyromagnetic ratio $\gamma$, gradient strength $G$, gradient duration $\delta$, and the time between the first and second diffusion gradients $\Delta$. The gyromagnetic ratio $\gamma$ for the proton is 42.576 MHz/T. In this experiment, $G$ was varied to obtain a list of different $b$ values (2.27, 16.86, 44.94, 86.53, 141.62, 210.22, 292.31, 389.92, 497.03, 619.63, 755.74, 907 $s/mm^2$). $\delta$ and $\Delta$ were kept constant at 0.006 s and 0.01 s respectively. The ADC map of the tomato was calculated by fitting Eq. (1) to the obtained $S$ of each voxel in the image and the $b$ values using MatLab 2010a (The Mathworks, Natick, MA). The resolution of the ADC map is 0.5 mm × 0.5 mm.

To select distinct spatial regions of interest (ROI) in the ADC map, the polygon region of interest tool in MATLAB R2010a (The Mathworks, Natick, MA) was used. The ROIs included the pericarp, and the inner tissue (columella, placenta, septa and locular tissues) (Van de Poel et al., 2014). The intensity of each voxel in the ADC map is the $D$-value of the tomato tissue contained within the volume of the voxel. The mean $D$ value of each spatial region was calculated as the intensity of voxel within the selected regions in the map. Ten fruit were used for each of the 4 time points studied.

### 2.6. Statistical analysis

The average values were used in the analysis. Data were subjected to ANOVA; Least Significant Difference (LSD) values were used to calculate variance at $P = 0.05$ and Duncan's multiple range tests ($P < 0.05$) were calculated to assess significance.

## 3. Results and discussion

### 3.1. Effect of chilling on respiration, ethylene production, ion leakage and apparent diffusion co-efficient

The aim of this study was to examine the extent to which MRI could detect changes in chilled Micro-Tom tomato fruit. Based on our previous data using Micro-Tom (Luengwilai et al., 2012a), fruit were stored at 0 °C in the dark for 0 (control), 1, or 2 weeks, and the fruit that were chilled for 2 weeks were held for 1 week at 20 °C. The onset of CI was evaluated using changes in respiration, ethylene evolution and ion leakage (Table 1). One week of chilling increased all of these indicators to levels that were maintained during an additional week of cold-storage ($P < 0.05$). In fruit transferred to 20 °C after 2 weeks of chilling, the rate of respiration returned to that of the pre-chilling levels, ion leakage remained at the same elevated levels and ethylene production continued to increase. A sustained rise in ethylene production upon warming after chilling is characteristic many chilling sensitive tissue (Saltveit, 2000; Luengwilai and Beckles, 2010).

MRI provided data that allowed the spatial resolution of the internal changes in chilling-induced fruit that were not available using conventional methods. ADC maps of an equatorial section of a tomato are shown in Fig. 1a. These heat maps indicate changes in water mobility, which increased during and after chilling; presumably because of chilling-induced disintegration of membrane integrity. After chilling at 0 °C for one week, the amount of voxels in the entire fruit in the yellow-red range (high $D$ value) increased compared with that of the non-chilled fruit (Figure 1a). This general trend continued during two weeks of cold storage (Fig. 1a). However, when these fruit were transferred to 20 °C, the number of yellow-red voxels throughout the slice decreased in the pericarp, but less so in the center of the fruit.

Quantitative data (i.e., histograms with the mode of the frequency derived from these maps) better illustrate differences among tissues (Fig. 1b). When compared with the pericarp, the inner tissues showed higher signal frequencies at greater ADCs after 2 weeks refrigeration followed by room temperature storage relative to the controls (Fig. 1b).

$D$-values were calculated for the whole fruit in order to make comparisons with ethylene and respiration data obtained from whole fruit. These values were higher in one week-chilled fruit compared with other storage periods (Table 2). After two weeks at 0 °C and with further storage at 20 °C, the $D$-values were similar to the control (Fig. 1 and Table 2). An increase after 1 week of chilling was also observed in carbon dioxide, ethylene evolution, and ion leakage (Tables 1 and 2). However, while these criteria remained higher than those in the non-chilled control fruit, the $D$-values declined relative to those in the control (Table 2).

The mean $D$-values of distinct spatial regions of the fruit were then calculated. No changes from the control were recorded in the pericarp after chilling for 1 or 2 weeks at 0 °C (Table 2). However, after an additional week of storage at 20 °C, $D$-values decreased to levels observed in the non-chilled control. This may be indicative of the ability of marginally chilled tissue to repair the chilling-induced physiological damage that accumulated during chilling when warmed to non-chilling temperatures (i.e., 20 °C) (Lyons and Breidenbach, 1990). There was little correspondence between changes in these $D$-values and changes in membrane ion leakage values; which were both derived from pericarp tissue (Fig. 1; Table 1). Ion leakage increased after cold exposure while $D$-values did not. There was some variability in pericarp ADC-values as mentioned earlier; cold-stored fruit varied compared to those reconditioned at 20 °C (Tables 1 and 2). Even when percent membrane permeability in the pericarp was considered over shorter time intervals, e.g., 15, 25 min, etc., changes due to chilling were still asynchronous with pericarp $D$-values (data not shown).

For the interior columella and locular tissues, the $D$-values increased after 1 week of chilling and remained at this elevated level for the remainder of the storage period (Table 2). This response was significantly different from that of the pericarp. When the controls were compared to fruit kept in the cold for 1 and 2 weeks, $D$-values for interior tissue correlated reasonably well with changes in respiration and ethylene production (both are non-destructive measurements). However the inner fruit $D$-values showed an identical pattern to changes in ion leakage, which is a destructive assessment of pericarp changes (Tables 1 and 2). This suggests two

**Table 1**
Effect of chilling at 0 °C on the rate of respiration and ethylene production from whole fruit of Micro-Tom tomato, and on the rate of ion leakage from pericarp fruit segments.

| Storage duration at 0 °C | $CO_2$ respiration rate ($\mu g\ kg^{-1}\ s^{-1}$) | Ethylene evolution rate ($ng\ kg^{-1}\ s^{-1}$) | Ion leakage (%)* |
|---|---|---|---|
| 0 weeks | 242.4 ± 27.2[a] | 11.3 ± 1.1[a] | 16.05 ± 3.79[a] |
| 1 week | 405.6 ± 44.4[b] | 32.9 ± 1.9[b] | 26.23 ± 2.66[b] |
| 2 weeks | 355.2 ± 36.6[b] | 29.8 ± 3.9[b] | 27.50 ± 1.38[b] |
| 2 weeks + 1 week at 20 °C | 270.4 ± 25.1[a] | 52.2 ± 3.5[c] | 28.89 ± 1.28[b] |

[abc] Numbers with different letters in the same column are significantly different calculated using Duncan's multiple range tests ($P < 0.05$).
* The rate of ion leakage is expressed as a percent of the total (at 120 min) compared with that initially in pericarp fruit segments.

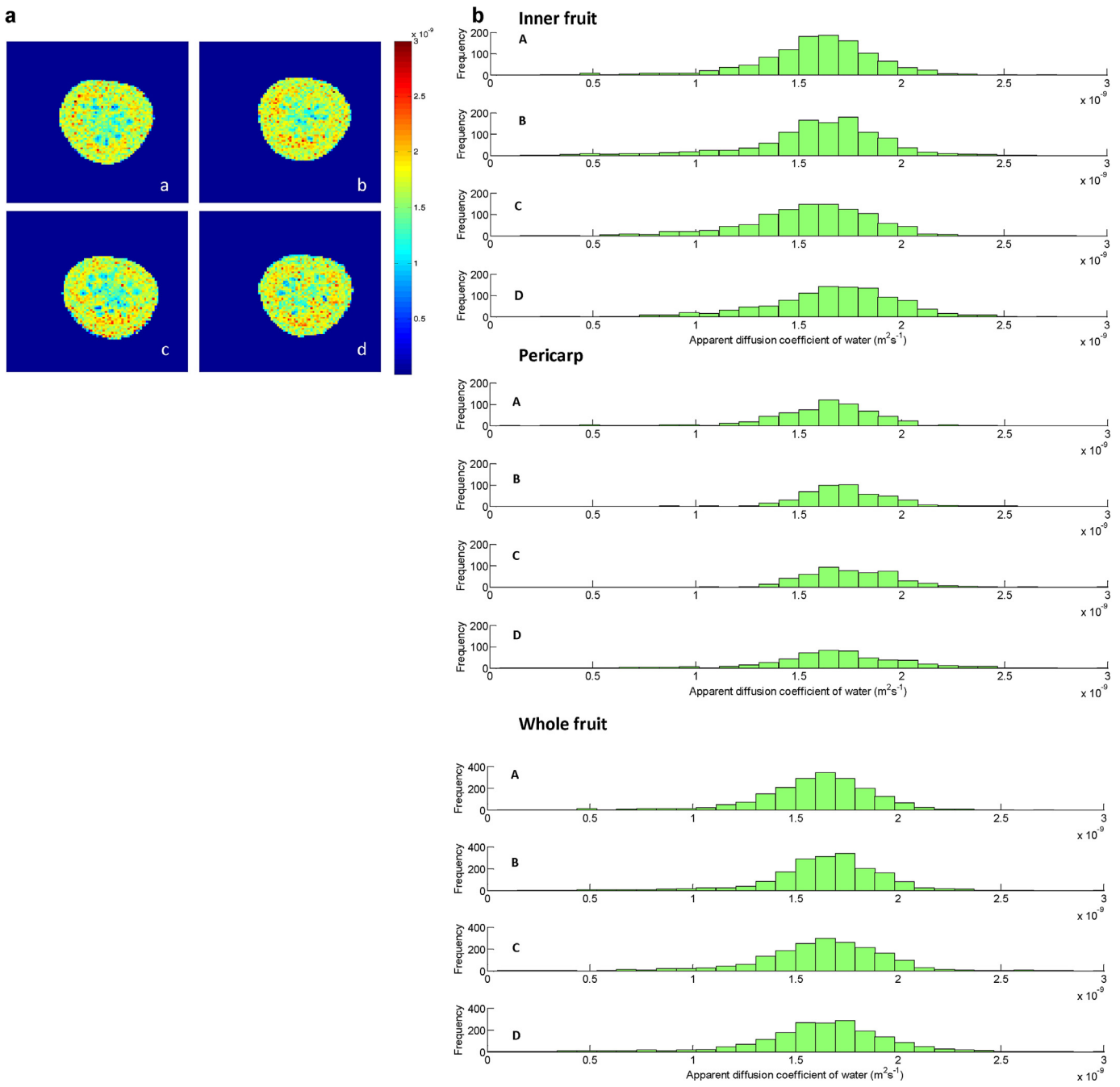


**Fig. 1.** (a) Apparent diffusion coefficient map of an equatorial slice of a single Micro-Tom tomato fruit. Each image shows the frequency of the signal (A) 0 week at 0 °C (non-chilled), (B) 1 week at 0 °C, (C) 2 weeks at 0 °C, (D) 2 weeks at 0 °C followed by 1 week at 20 °C. The *D* value of each fruit was calculated as the average of the *D*-values of all voxels in the fruit. The color scale is shown in the color bar. Voxels in red have high *D*-values, and voxels in blue indicate low *D*-values. (b) Histograms of the apparent diffusion coefficient map of an equatorial slice of a Micro-Tom tomato calculated from the pericarp, inner fruit (the columella and locular tissue) and the whole fruit. Each bar shows the frequency of the signal (A) 0 week at 0 °C (non-chilled), (B) 1 week at 0 °C, (C) 2 weeks at 0 °C, (D) 2 weeks at 0 °C followed by 1 week at 20 °C. Please note that the scale for the pericarp and inner tissues vary from that for the whole fruit. (For interpretation of the references to color in this figure legend, the reader is referred to the web version of this article.)

**Table 2**
Effect of chilling on the apparent diffusion coefficient (D) of water in tomato fruit after storage at 0 °C over different time periods.

| Storage duration at 0 °C | *D* (whole fruit) ($\times 10^{-9}$ m$^2$ s$^{-1}$) | *D* (pericarp) ($\times 10^{-9}$ m$^2$ s$^{-1}$) | *D* (inner fruit)* ($\times 10^{-9}$ m$^2$ s$^{-1}$) |
|---|---|---|---|
| 0 week | 1.600[b] | 1.660[ab] | 1.553[b] |
| 1 week | 1.644[a] | 1.703[a] | 1.608[a] |
| 2 week | 1.640[ab] | 1.707[a] | 1.606[a] |
| 2 week + 1 week at 20 °C | 1.639[ab] | 1.627[b] | 1.643[a] |

[ab] Numbers with different letters in the same column are significantly different calculated using Duncan's multiple range tests ($P < 0.05$).
* Inner fruit indicates the columella and locular tissue.

possibilities: (1) that each individual assay acts as a proxy for similar underlying biological processes, but that they each encapsulate some divergent mechanisms, or (2) that in response to cold, the pericarp and inner fruit may be modulated in different temporal timeframes with varying amplitudes.

### 3.2. Implications of this work

Membrane disintegration and the subsequent physiological changes in chilled fruit may promote higher water mobility detected as increased *D*-values. Interpretation of these data suggest that the sensitivity and responsiveness to chilling differs between the pericarp and core tissues. This may arise due to the physical distance from the epidermis to the fruit center. An endogenous temperature gradient may be imposed across the fruit creating an inherent delay in the response and any subsequent adaptation to cold, between pericarp and core tissues. Although this possibility cannot be ruled out, the relatively small diameter of Micro-Tom fruit should minimize this effect. Of more importance may be the heterogeneous nature of the fruit tissues. Differences in their physiochemical properties and functionalities could produce different biological outcomes to chilling. The realization that fruit responses to cold are asynchronous should inform our view when designing and interpreting data from experiments to study chilling injury.

The aim of the experiments described here was to explore basic fruit postharvest biology using MRI and thereby gain new insight into CI. While not fast enough for commercial use, the MRI scan time of 27 min were still much faster than the more than 3 h needed to measure respiration, ethylene evolution and ion leakage. In addition to being faster, MRI also provides spatially resolved data. A long-term goal would be to refine this technology to enable its practical application as an economical, robust and rapid on-line detector of postharvest disorders in packinghouses or even along the supply chain. This would allow each stakeholder to have better control over produce quality. Examining the response of different cultivars that vary in fruit size, pericarp thickness, ratio of columella to locular tissues, and sugar to acid content, and to a variety of low temperature incubations will also be necessary to facilitate MRI's adoption in commercial settings.

## 4. Conclusions

Unlike measurements of ion leakage, respiration and ethylene production that are commonly used in the study of physiological changes associated with chilling injury, MRI provided non-invasive, spatially resolved data within different tissues of the fruit. There were no detectable changes in *D*-values in the pericarp after chilling compared to the control. In contrast, the columella and locular *D*-values increased upon chilling (Table 2). These data suggest that the disruption of some physiological and biochemical processes caused by chilling may vary in their timing and intensity in the inner tissues of the fruit compared to the pericarp. This may point to the need to be more cautious when extrapolating data obtained from measurements of pericarp to physiological events occurring in the whole fruit.

## Acknowledgements

We thank Ms. Karin Albornoz and the anonymous reviewers for their critical evaluation of this manuscript and for suggesting helpful improvements. This work was supported by Hatch Funds CA-D-PLS-7821-H (DMB). The Zhejiang Association for International Exchange of Personnel supported FT.

## References

Abbott, J.A., 1999. Quality measurement of fruits and vegetables. Postharvest Biol. Technol. 15, 207–225.
Barreiro, P., Ruiz-Cabello, J., Fernandez-Valle, M.E., Ortiz, C., Ruiz-Altisent, M., 1999. Mealiness assessment in apples using MRI techniques. Magn. Reson. Imaging 17, 275–281.
Beckles, D.M., Hong, N., Stamova, L., Luengwilai, K., 2012. Biochemical factors contributing to tomato fruit sugar content: a review. Fruits 67, 49–64.
Clark, C.J., Forbes, S.K., 1994. Nuclear-Magnetic-Resonance Imaging of the Development of Chilling Injury in Fuyu Persimmon (Diospyros-Kaki). New Zealand J. Crop Hortic. Sci. 22, 209–215.
Clark, C.J., Hockings, P.D., Joyce, D.C., Mazucco, R.A., 1997. Application of magnetic resonance imaging to pre- and post-harvest studies of fruits and vegetables. Postharvest Biol. Technol. 11, 1–21.
Defraeye, T., Lehmann, V., Gross, D., Holat, C., Herremans, E., Verboven, P., Verlinden, B.E., Nicolai, B.M., 2013. Application of MRI for tissue characterisation of 'Braeburn' apple. Postharvest Biol. Technol. 75, 96–105.
Gomez, P., Ferrer, M.A., Fernandez-Trujillo, J.P., Calderon, A., Artes, F., Egea-Cortines, M., Weiss, J., 2009. Structural changes, chemical composition and antioxidant activity of cherry tomato fruits (cv, Micro-Tom) stored under optimal and chilling conditions. J. Sci. Food Agric. 89, 1543–1551.
Gonzalez, J.J., Valle, R.C., Bobroff, S., Viasi, W.V., Mitcham, E.J., McCarthy, M.J., 2001. Detection and monitoring of internal browning development in 'Fuji' apples using MRI. Postharvest Biol. Technol. 22, 179–188.
Herremans, E., Melado-Herreros, A., Defraeye, T., Verlinden, B., Hertog, M., Verboven, P., Val, J., Fernandez-Valle, M.E., Bongaers, E., Estrade, P., Wevers, M., Barreiro, P., Nicolai, B.M., 2014. Comparison of X-ray CT and MRI of watercore disorder of different apple cultivars. Postharvest Biol. Technol. 87, 42–50.
Hertog, M.L.A.T.M., Lammertyn, J., Desmet, M., Scheerlinck, N., Nicolai, B., 2004. The impact of biological variation on postharvest behaviour of tomato fruit. Postharvest Biol. Technol. 34, 271–284.
Lammertyn, J., Dresselaers, T., Van Hecke, P., Jancsok, P., Wevers, M., Nicolai, B.M., 2003. MRI and X-ray CT study of spatial distribution of core breakdown in 'Conference' pears. Magn. Reson. Imaging 21, 805–815.
Letal, J., Jirak, D., Suderlova, L., Hajek, M., 2003. MRI 'texture' analysis of MR images of apples during ripening and storage. Lebensm. Wiss. Technol. 36, 719–727.
Luengwilai, K., Beckles, D.M., 2010. Climacteric ethylene is not essential for initiating chilling injury in tomato (*Solanum lycopersicum*) cv. Ailsa Craig. J. Stored Prod. Postharvest Res. 1, 1.
Luengwilai, K., Beckles, D.M., Saltveit, M.E., 2012a. Chilling-injury of harvested tomato (*Solanum lycopersicum* L.) cv, Micro-Tom fruit is reduced by temperature pre-treatments. Postharvest Biol. Technol. 63, 123–128.
Luengwilai, K., Saltveit, M., Beckles, D.M., 2012b. Metabolite content of harvested Micro-Tom tomato (*Solanum lycopersicum* L.) fruit is altered by chilling and protective heat-shock treatments as shown by GC-MS metabolic profiling. Postharvest Biol. Technol. 63, 116–122.
Lyons, J.M., 1973. Chilling injury in plants. Annu. Rev. Physiol. 24, 445–466.
Lyons, J.M., Breidenbach, R.W., 1990. Relation of Chilling Stress to Respiration. CRC Press, Boca Raton, FL.
Malacrida, C., Valle, E.M., Boggio, S.B., 2006. Postharvest chilling induces oxidative stress response in the dwarf tomato cultivar Micro-Tom. Physiol. Plant. 127, 10–18.
Meissner, R., Jacobson, Y., Melamed, S., Levyatuv, S., Shalev, G., Ashri, A., Elkind, Y., Levy, A.A., 1997. A new model system for tomato genetics. Plant J. 12, 1465–1472.
Morris, L.L., 1982. Chilling injury of horticultural crops – an overview. Hortscience 17, 161–162.
Nicolai, B., Defraeye, T., De Ketelaere, B., Herremans, E., Hertog, M.L.T.M., Saeys, W., Torricelli, A., Vandendriessche, T., Verboven, P., 2014. Nondestructive measurements of fruit and vegetable quality. Ann. Rev. Food Sci. Technol. 5, 285–312.
Re, M.D., Gonzalez, C., Sdrigotti, M.A., Sorrequieta, A., Valle, E.M., Boggio, S.B., 2012. Ripening tomato fruit after chilling storage alters protein turnover. J. Sci. Food Agric. 92, 1490–1496.
Saltveit, M.E., 1991. Prior temperature exposure affects subsequent chilling sensitivity. Physiol. Plant. 82, 529–536.
Saltveit, M.E., 2000. Discovery of chilling injury. In: Kung, S.D., Yang, S.F. (Eds.), Discoveries in Plant Biology. World Scientific Publishing Co., Singapore, pp. 423–448.
Saltveit, M.E., 2002. The rate of ion leakage from chilling-sensitive tissue does not immediately increase upon exposure to chilling temperatures. Postharvest Biol. Technol. 26, 295–304.
Saltveit, M.E., 2003. Temperature extremes. In: Bartz, J.A., Brecht, J.K. (Eds.), Postharvest Physiology and Pathology of Vegetables. Marcel Dekker, New York, pp. 457–484.
Saltveit, M.E., 2005. Influence of heat shocks on the kinetics of chilling-induced ion leakage from tomato pericarp discs. Postharvest Biol. Technol. 36, 87–92.
Saltveit, M.E., Strike, T., 1989. A rapid method for accurately measuring oxygen concentrations in milliliter gas samples. Hortscience 24, 145–147.
Seymour, G.B., Chapman, N.H., Chew, B.L., Rose, J.K.C., 2013. Regulation of ripening and opportunities for control in tomato and other fruits. Plant Biotechnol. J. 11, 269–278.
Sharom, M., Willemot, C., Thompson, J.E., 1994. Chilling injury induces lipid phase-changes in membranes of tomato fruit. Plant Physiol. 105, 305–308.

Sorrequieta, A., Abriata, L.A., Boggio, S.B., Valle, E.M., 2013. Off-the-vine ripening of tomato fruit causes alteration in the primary metabolite composition. Metabolites 3, 967–978.

Van de Poel, B., Vandenzavel, N., Smet, C., Nicolay, T., Bulens, I., Mellidou, I., Vandoninck, S., Hertog, M.L.A.T.M., Derua, R., Spaepen, S., Vanderleyden, J., Waelkens, E., De Proft, M.P., Nicolai, B.M., Geeraerd, A.H., 2014. Tissue specific analysis reveals a differential organization and regulation of both ethylene biosynthesis and E8 during climacteric ripening of tomato. BMC Plant Biol. 14.

Vega-Garcia, M.O., Lopez-Espinoza, G., Ontiveros, J.C., Caro-Corrales, J.J., Vargas, F.D., Lopez-Valenzuela, J.A., 2010. Changes in protein expression associated with chilling injury in tomato fruit. J. Am. Soc. Hortic. Sci. 135, 83–89.

Wang, C.Y., Wang, P.C., 1992. Differences in nuclear-magnetic-resonance images between chilled and nonchilled Zucchini Squash. Environ. Exp. Bot. 32, 213–219.

Weiss, J., Egea-Cortines, M., 2009. Transcriptomic analysis of cold response in tomato fruits identifies dehydrin as a marker of cold stress. J. Appl. Genet. 50, 311–319.

Zhang, L., McCarthy, M.J., 2012. Measurement and evaluation of tomato maturity using magnetic resonance imaging. Postharvest Biol. Technol. 67, 37–43.